the FEBS Journal

New insights into the functions and *N*-glycan structures of factor X activator from Russell's viper venom

Hong-Sen Chen[1], Jin-Mei Chen[2], Chia-Wei Lin[1], Kay-Hooi Khoo[1,2] and Inn-Ho Tsai[1,2]

1 Graduate Institute of Biochemical Sciences, National Taiwan University, Taiwan
2 Institute of Biological Chemistry, Academia Sinica, Taipei, Taiwan

Keywords
cDNA cloning; factor X activator; glycan mass spectrometry; Lewis and sialyl-Lewis; Russell's viper venom

Correspondence
I. H. Tsai, Institute of Biological Chemistry, Academia Sinica, PO Box 23-106, Taipei, Taiwan
Fax: 886 22 3635038
Tel: 886 22 3620264
E-mail: bc201@gate.sinica.edu.tw

(Received 18 February 2008, revised 22 April 2008, accepted 5 June 2008)

doi:10.1111/j.1742-4658.2008.06540.x

The coagulation factor X activator from Russell's viper venom (RVV-X) is a heterotrimeric glycoprotein. In this study, its three subunits were cloned and sequenced from the venom gland cDNAs of *Daboia siamensis*. The deduced heavy chain sequence contained a C-terminal extension with four additional residues to that published previously. Both light chains showed 77–81% identity to those of a homologous factor X activator from *Vipera lebetina* venom. Far-western analyses revealed that RVV-X could strongly bind protein S, in addition to factors X and IX. This might inactivate protein S and potentiate the disseminated intravascular coagulation syndrome elicited by Russell's viper envenomation. The *N*-glycans released from each subunit were profiled and sequenced by MALDI-MS and MS/MS analyses of the permethyl derivatives. All the glycans, one on each light chain and four on the heavy chain, showed a heterogeneous pattern, with a combination of variable terminal fucosylation and sialylation on multiantennary complex-type sugars. Amongst the notable features were the presence of terminal Lewis and sialyl-Lewis epitopes, as confirmed by western blotting analyses. As these glyco-epitopes have specific receptors in the vascular system, they possibly contribute to the rapid homing of RVV-X to the vascular system, as supported by the observation that slower and fewer fibrinogen degradation products are released by desialylated RVV-X than by native RVV-X.

Activators for zymogens of the blood coagulation cascade are abundant in venoms of many Viperinae [1] and some Elapidae [2,3]. The factor X activator from the venom of Russell's viper (*Daboia russelli* and *Daboia siamensis*) (RVV-X) is a potent procoagulating and lethal toxin [4]. Its action mechanism involves the Ca^{2+}-dependent hydrolysis of the peptide bond between Arg51 and Ile52 of the heavy chain on factor X, similar to the physiological activation by factors IXa and VIIa [4,5]. In addition, RVV-X also activates factor IX, but not prothrombin [6]. Given these functional specificities, RVV-X has served as a tool for thrombosis research and as a diagnostic reagent [7].

RVV-X is a heterotrimeric glycoprotein composed of one heavy chain (HC) and two distinct light chains (LC1 and LC2) [8,9]. The heavy chain is a P-III metalloprotease [10], and both light chains belong to the C-type lectin-like family. However, the light chain LC2 has yet to be fully sequenced [8]. Based on their sequence similarity to other venom factor IX/X-binding proteins [8,11], both light chains of RVV-X have

Abbreviations
APTT, activated partial thromboplastin time; DIC, disseminated intravascular coagulation; FDP, fibrinogen degradation product; Gla, γ-carboxyglutamic acid; PNGase F, peptide *N*-glycosidase F; PVDF, poly(vinylidene difluoride); RVV-X, factor X activator from Russell's viper venom; SBHP, streptavidin-biotinylated horseradish peroxidase; TBST, Tris-buffered saline with Tween 20; VAP1, vascular apoptosis-inducing protein 1; VLFXA, factor X activator from *Vipera lebetina* venom.

been postulated to bind the γ-carboxyglutamic acid (Gla) domain of factor X and bring the heavy chain to the Arg51 cleavage site of factor X [4]. This speculation has been supported by a recent crystallographic study of RVV-X at 2.9 Å resolution [12]. In addition, a homologous factor X activator from *Vipera lebetina* venom (VLFXA) has been characterized, and its three subunits have been cloned and fully sequenced [13,14]. Its heavy chain and light chain LC1 share high sequence similarity (> 77%) to those of RVV-X.

The structures of the carbohydrate moieties of RVV-X have been investigated previously. It was found that RVV-X contains multiantennary complex-type N-glycans, with bisecting GlcNAc and terminal Neu5Acα2–3Gal sialylation. The glycan core structures were additionally shown to be sufficient to maintain the active conformation of RVV-X [9,15]. However, details on the glycosylation and physiological significance of these glycans remain to be explored. In this study, we have cloned all the RVV-X subunits for the first time and have solved their complete sequences. The nucleotide sequences of HC, LC1 and LC2 have been deposited in GenBank with accession numbers DQ137799, AY734997 and AY734998, respectively. The overall N-glycosylation profiles, as well as that of the individual subunits and sites, were defined by advanced mass spectrometry analyses. Unexpectedly, terminal fucosylation contributing to Lewis (Le) and sialyl-Lewis (SLe) epitopes was also identified, and their functional implications were clarified by *in vivo* studies.

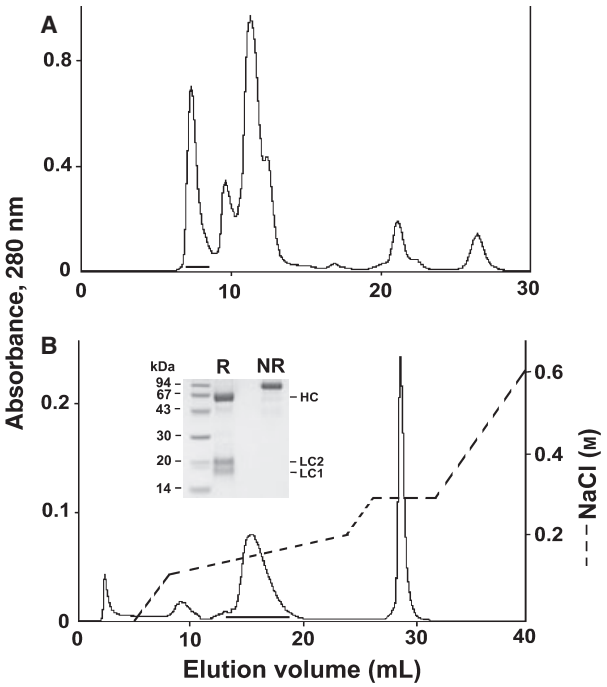

Fig. 1. Purification of RVV-X. (A) About 20 mg of *D. siamensis* venom was dissolved in buffer and separated by Superdex G-75 gel filtration. The column was equilibrated and eluted with 100 mM ammonium acetate (pH 6.7). Fraction I (indicated by bar) possessing coagulation activity was pooled and lyophilized. (B) Subsequent purification of fraction I on a Mono Q column. The elution was achieved by increasing (0–0.6 M) NaCl gradient in 50 mM Tris/HCl, pH 8.0. The absorbance at 280 nm of the eluent was monitored online. The inset shows the result of SDS-PAGE of purified RVV-X under reducing (R) and nonreducing (NR) conditions.

Results and Discussion

Purification and characterization of RVV-X

RVV-X was purified from the crude venom of *D. siamensis* (Flores Island, Indonesia) by two chromatographic steps. The venom was separated into seven fractions using a Superdex G-75 column (Fig. 1A). The first peak (indicated by a bar) exhibiting strong procoagulating activity was further purified by anion exchange chromatography (Fig. 1B). The yield of RVV-X was approximately 3.4% (w/w) of the crude venom, similar to that reported previously [4]. SDS-PAGE of the purified protein revealed a single band at 93 kDa under nonreducing conditions, and three bands of 62, 21 and 18 kDa under reducing conditions (Fig. 1B, inset). The molecular mass of purified RVV-X was also determined by an analytical ultracentrifuge as 92 972 ± 4356 Da (data not shown). After electrophoresis and blotting, the protein band of LC2 was excised from the poly(vinylidene difluoride) (PVDF) membrane. By automatic Edman sequencing, its N-terminal sequence 1–25 was determined as LDXPPDSSLYRYFXYRVFKEHKT (X denotes an unidentified residue), which differs from that of VLFXA LC2 by three residues at positions 10, 22 and 24 [14].

The stability of RVV-X under various conditions was studied by activated partial thromboplastin time (APTT) coagulation assay. We first assigned a plot of clotting time against dose of RVV-X that fitted well in a power regression mode (Fig. 2A). On the basis of this relationship, we determined the remaining activities after different treatments. The results showed that RVV-X was stable in buffers of pH 6–10 and temperatures below 37 °C (Fig. 2B,C), consistent with previous studies showing that purified RVV-X was stable at 4 °C in 50 mM $Tris/H_3PO_4$ buffer, pH 6.0 for 2 months [16]. These properties were also similar to those of the P-III metalloproteinase VAP1 (vascular apoptosis-inducing protein 1) from *Crotalus atrox* venom [17].

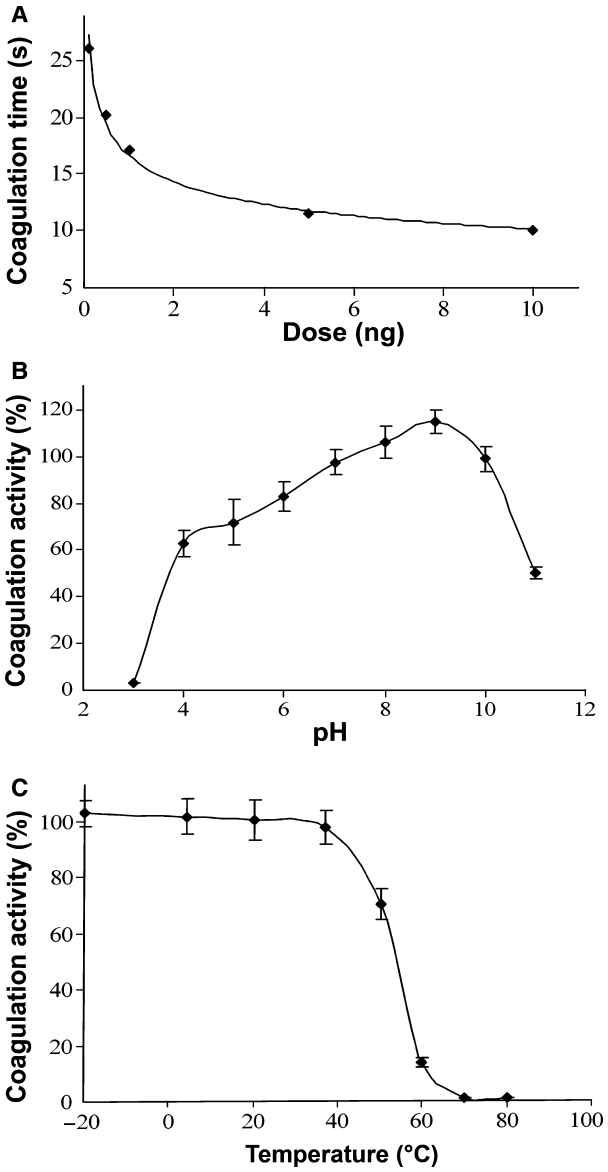

Fig. 2. Effects of buffer pH and temperature on the coagulation activity of RVV-X. (A) Relationship between the clotting time and dose of RVV-X in APTT coagulation assay. Analysing the experimental data (0.1–10 ng) with power regression gives a correlation of $R^2 = 0.991$ and a prediction equation of $y = 16.624x^{-0.2148}$. (B) pH stability profile. RVV-X (1 $\mu g \cdot \mu L^{-1}$) was incubated at 4 °C for 36 h in buffers of different pH. (C) Thermal stability profile. RVV-X (1 $\mu g \cdot \mu L^{-1}$ in 100 mM Hepes, pH 8.0) was incubated at various temperatures for 1 h. The remaining activities of 5 ng of RVV-X after (B) and (C) treatments were evaluated by the coagulation assay. The results are expressed as the mean ± standard deviation ($n = 3$).

Substrate specificities studied by far-western analysis

To investigate the binding specificity of RVV-X, several human coagulation factors containing the Gla domain were subjected to SDS-PAGE (Fig. 3A) and then electroblotted onto a PVDF membrane. The blot was incubated with biotinylated RVV-X, and binding was detected with the streptavidin-biotinylated horseradish peroxidase (SBHP) system (Fig. 3B,C). In the presence of a millimolar concentration of Ca^{2+} ions, RVV-X bound strongly to factors X and IX, whereas its binding to prothrombin and protein C was hardly detectable. When Ca^{2+} ions were removed from the solution, binding was no longer detectable (Fig. 3C), confirming that exogenous Ca^{2+} ions are essential for substrate binding [18]. Furthermore, no signal could be detected for factor X without the Gla domain (Fig. 3B, lane 7).

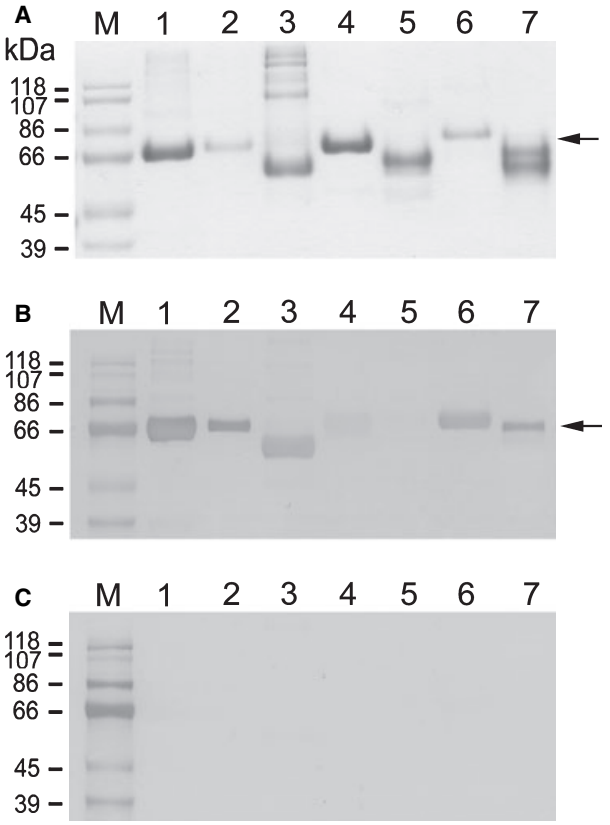

Fig. 3. Analysis of the binding of RVV-X to Gla-containing plasma factors or proteins by far-western blotting. (A) Coagulation factors were separated by SDS-PAGE and stained by Coomassie brilliant blue G-250. Lane 1, 3 μg of factor X; lane 2, 0.3 μg of factor X; lane 3, 3 μg of factor IX; lane 4, 3 μg of prothrombin; lane 5, 3 μg of protein C; lane 6, 3 μg of protein S; lane 7, 3 μg of Gla-domainless factor X. (B) Instead of staining, the protein bands were blotted on to a PVDF membrane after PAGE. The membrane was probed with 1.5 $\mu g \cdot mL^{-1}$ biotinylated RVV-X and detected with the SBHP system in the presence of 5 mM $CaCl_2$. (C) Same as (B), except Ca^{2+} ions were excluded. For lane 7, the arrow denotes residual factor X present in the sample of Gla-domainless factor X.

Thus, the far-western results reflect the substrate specificity of RVV-X [4,6], and its binding to substrates involves their Gla domains [19]. Interestingly, we found that protein S bound strongly to RVV-X (Fig. 3B, lane 6). If RVV-X inactivates protein S *in vivo*, it will interrupt the protein C pathway [20] and stimulate the tissue factor pathway [21], both of which may lead to an increase in the risk of coagulation and disseminated intravascular coagulation (DIC) syndrome.

Cloning and sequence alignment of RVV-X subunits

PCR amplification and cloning of the light chains of RVV-X were carried out using cDNA prepared from venom glands of *D. siamensis* (Flores Island, Indonesia) as template. After RT-PCR, 20 clones encoding C-type lectin-like proteins were sequenced. Of these, 10 clones were found to encode the LC2 and LC1 subunits. Others were found to encode other variants of the C-lectin-like venom proteins. The amino acid sequences of both subunits were deduced from the nucleotide sequences, and were found to match the N-terminal sequences of the corresponding proteins [8]. The ORF of LC2 encodes a precursor of 158 amino acids, including a signal peptide of 23 residues and mature protein of 135 residues. Its predicted mass is 15 983 Da, its isoelectric point is 5.44 and it has a potential *N*-glycosylation site at Asn59. The LC1 precursor contains 146 amino acids, including a signal peptide of 23 residues, and the predicted sequence for its mature protein matches that published previously [8].

The amino acid sequences of LC1 and LC2, together with those of other homologues of factor IX/X-binding lectin-like subunits, are aligned in Fig. 4. They show the highest sequence identity (77–81%) to the corresponding subunits of VLFXA [14]. Residues Glu100 and Arg102 of LC2, presumably important for interacting with the Gla domain of factor X [19], were conserved in both LC2 subunits of RVV-X and VLFXA. In addition to the conserved Cys residues present in this lectin-like family, both LC2 subunits contain an extra Cys at the extended C-terminus, which probably forms an interchain disulfide bridge with the heavy chain [14]. LC1 is covalently linked to LC2 but not to the heavy chain.

The crystal structures of the factor IX/X-binding lectin-like proteins from pit viper venom revealed that each subunit contained one Ca^{2+}-binding site and four corresponding residues that coordinated Ca^{2+} ions [22]. It was shown later that only one subunit of factor IX/X-binding protein from *Echis* venom had a Ca^{2+}-binding site; the other non-Ca^{2+}-binding subunit was stabilized by C-terminal Lys/Arg residues [23]. We found that the LC2 and LC1 sequences of RVV-X (Fig. 4) lacked the Ca^{2+}-binding acidic residues found in the sequences of crotalid factor IX/X-binding proteins; instead, they contained basic residues at these

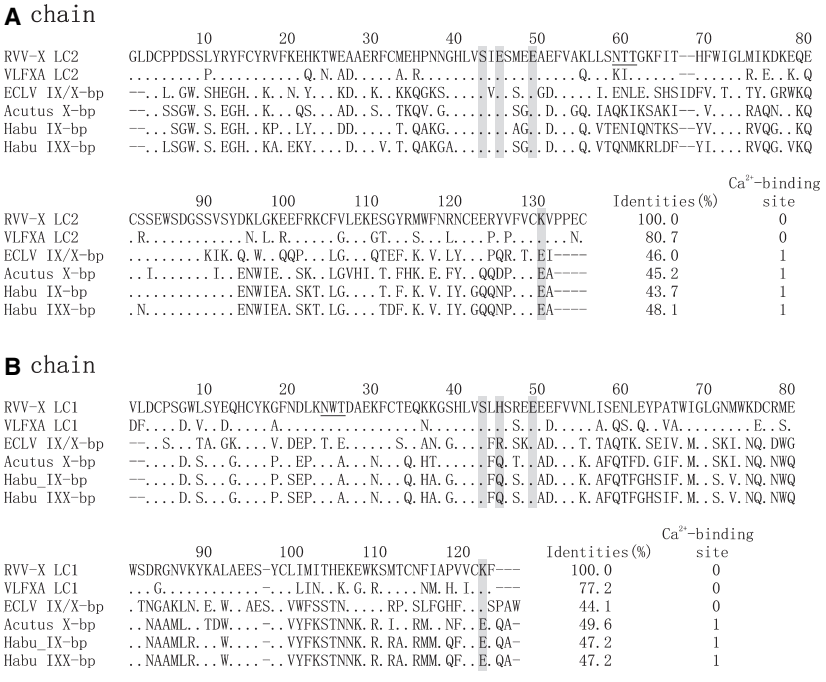

Fig. 4. Sequence alignments of RVV-X light chains with other factor IX/X-binding proteins. Residues identical to those of LC2 and LC1 are denoted with dots; gaps are marked with hyphens. Putative Ca^{2+}-binding sites and potential N-glycosylation sites are shown in grey and underlined, respectively. Accession numbers and venom species are as follows: VLFXA LC2 (AY57811) and LC1 (AY339163), *Macrovipera lebetina*; ECLV IX/X-bp α subunit (AAB36401) and β subunit (AAB36402), *Echis leucogaster*; Acutus X-bp A chain (1IODA) and B chain (1IODB), *Deinagkistrodon acutus*; Habu IX/X-bp A chain (P23806) and B chain (P23807), Habu X-BP A chain (1J34A) and B chain (1J34B), *Protobothrops flavoviridis*.

sites. This may reflect an evolutionary difference between Viperinae and Crotalinae venoms in the structure of factor IX/X-binding protein families.

Using similar procedures, cDNA encoding the RVV-X heavy chain (RVV-X HC) was cloned and sequenced. Its ORF encodes a P-III precursor protein of 619 amino acids, including a 188-residue highly conserved proenzyme domain followed by a mature protein of 431 residues (Fig. 5), consistent with its published protein sequence [8]. The proenzyme domain contains a 'cysteine switch' motif (PKMCGVT), which is possibly required for its processing and activation. Notably, the predicted RVV-X HC contains a C-terminal extension of four additional residues (FSQI). Whether this implies post-translational processing or geographical variations amongst *D. siamensis* venoms is not clear. A similar phenomenon has been reported for the deduced protein sequence of HR1b, which has an additional seven residues (TTVFSLI) at the C-terminus, and proteolytic processing was suggested to have occurred [24].

Figure 5 shows the alignment of the amino acid sequences of RVV-X HC with those of other representative P-III enzymes. It shows highest similarity (82%) to VLFXA HC, and lower similarity to other P-III proteases, e.g. Ecarin (63%), Daborhagin (56%), HR1b (54%) and VAP1 (53%). The proenzyme domain, zinc-chelating motif, methionine turn and three potential Ca^{2+}-binding sites are all conserved (Fig. 5). Notably, residue Cys562, which presumably forms a disulfide bond with Cys135 of LC2, is located within the highly variable region, which is important for substrate recognition of the A disintegrin and metalloproteinase (ADAM) family [25]. By this unique linking to RVV-X HC, the light chains appear to confer the substrate specificities of RVV-X [12]. Collectively, the primary sequences of the three subunits of RVV-X (Figs 4 and 5) suggest the possible presence of three conformational Ca^{2+}-binding sites in the heavy chain and none in LC1 and LC2, in accordance with the results of its crystallographic structure [12].

N-glycosylation profiles

The isolation of the individual heavy and light chains in sufficient yield allowed a detailed structural characterization of their respective N-glycosylation profiles to be performed. Previous investigation based primarily on lectin binding, sialidase treatment, glycosyl composition and linkage analyses has led to the conclusion that the N-glycans of RVV-X are mostly of the complex type, with bisecting GlcNAc and α2–3Neu5Ac sialylation on a proportion of terminal β-Gal residues as the most notable structural features [9]. More specifically, it was estimated that about 5% of the total N-glycans are of high mannose type, 65% are of biantennary complex type and 30% are of tri-/tetra-antennary complex type. On the basis of interactions with immobilized erythroagglutinating phytohaemagglutinin lectin, 50–60% of the total glycans are deduced to carry a bisecting GlcNAc, consistent with the detection of a substantial amount of 3,4,6-Man in a ratio of $\sim 2:1$ relative to nonbisected 3,6-Man by methylation analysis. Approximately 0.5–0.8 mol of terminal Fuc was also detected per 3 mol of Man (1 mol of *N*-glycan), but the exact location was not defined as the expected 4,6-linked GlcNAc residue, corresponding to the reducing end GlcNAc in which core fucosylation is normally attached, could not be identified. This overall picture is mostly reproduced in our current analysis based on MALDI-MS (Fig. 6) and advanced MS/MS (Fig. 7) analyses of the permethylated N-glycans, but with a few important new findings.

Overall, the salient structural characteristics of the N-glycans released from the heavy and light chains are similar. However, a major signal corresponding to the high-mannose-type $Man_5GlcNAc_2$ structure was only found in the heavy chain. In addition, there is a relatively higher abundance of the larger size, multiantennary glycans carried on the heavy chain, which gave a much more heterogeneous and complex profile. As listed in Table 1, the assigned compositions for the major $[M + Na]^+$ molecular ion signals detected correspond to the expected complex-type N-glycans with up to five Hex-HexNAc units. The majority carry a variable degree of Neu5Ac sialylation and an extra HexNAc residue that is attributable to the bisecting GlcNAc. Importantly, some of the larger structures were found to contain more than one Fuc residue, giving a first indication that not all fucosylation can be ascribed to core α6-fucosylation. Core α3-fucosylation was ruled out as these N-glycans were released by peptide *N*-glycosidase F (PNGase F). It is thus likely that some or all of the Fuc residues may be attached to the terminal sequences.

As shown by MALDI-TOF/TOF MS/MS analyses of representative Fuc-containing major N-glycans (Fig. 7), the trimannosyl core structures are indeed bisected by GlcNAc and are nonfucosylated. Fuc was found to be attached to the 3-position of HexNAc of the terminal Hex-HexNAc unit, giving rise to the Le^x epitope and SLe^x when additionally sialylated. The characteristic D ions for Le^x and SLe^x were detected at m/z 472 and 833, respectively, whereas the corresponding ion indicative of Le^a and SLe^a at m/z 442 was either not found or was too minor to allow

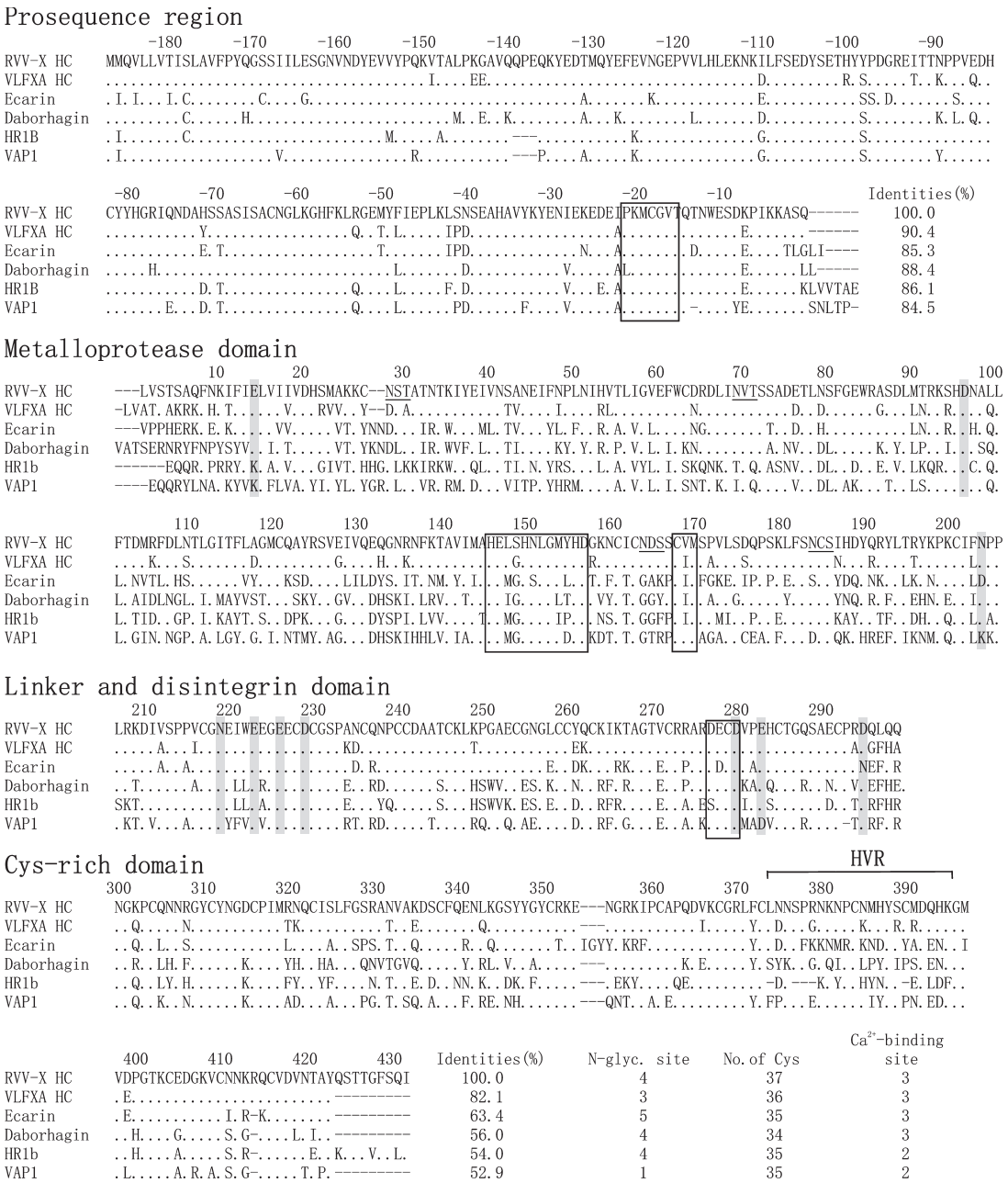

Fig. 5. Sequence alignments of RVV-X heavy chain with other P-III enzymes. Residues identical to those of RVV-X HC are denoted by dots, and gaps are marked with hyphens. Putative Ca^{2+}-binding sites and potential *N*-glycosylation sites are shown in grey or underlined, respectively. Conserved cysteine switch, zinc-binding site, methionine turn and ECD motif are boxed. Accession numbers and venom species are as follows: VLFXA HC (AAQ17467), *Macrovipera lebetina*; Ecarin (Q90495), *Echis carinatus*; Daborhagin (DQ137798), *D. russelli*; HR1b (BAB92014), *Protobothrops flavoviridis*; VAP1 (BAB18307), *Crotalus atrox*.

unambiguous identification. Other terminal epitopes include the nonsubstituted Hex-4HexNAc (Galβ1–4GlcNAcβ1-, LacNAc), Neu5Acα2–3Hex-4HexNAc and nonextended terminal HexNAc residues. The presence of bisecting GlcNAc was established from several complementary ion series. First, the D ion formed at the bisected 3,4,6-linked β-Man residue carried the extra bisecting GlcNAc residue together with the 6-arm substituents. Second, a characteristic loss of both the bisecting GlcNAc and the 3-arm substituents, in concert with a ^{1,5}A-type ring cleavage at the β-Man residue, yielded an ion at 321 mass units lower than

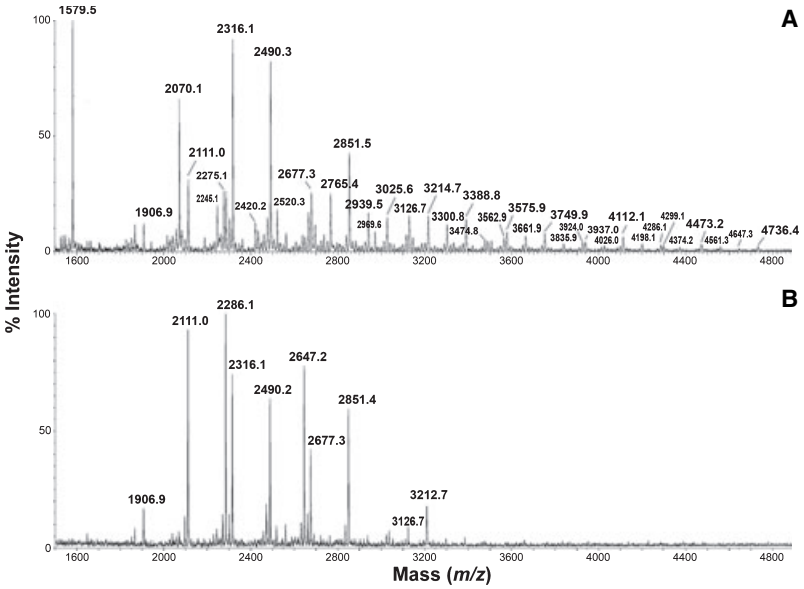

Fig. 6. MALDI-MS profiling of the N-glycans. N-glycans released from the heavy chain (A) and LC1 (B) of RVV-X were permethylated and profiled by MALDI-MS. The N-glycans of LC1 and LC2 gave similar profiles, and only that of LC1 is shown here. The molecular composition assignments of the major signals detected are listed in Table 1, several of which were further analysed by MS/MS to deduce the terminal epitopes carried and their probable structures.

the corresponding D ion. Third, the ^{0,4}A ion would include the 6-arm substituents, but not the extra GlcNAc residue, if the latter bisects the β-Man residue at the C4 position. Finally, an H ion would be formed through concerted loss of the substituents on the 6-arm and the bisecting GlcNAc.

The identification of Le^x and SLe^x by MS/MS sequencing was further corroborated by western blot analyses (Fig. 8) using a panel of specific monoclonal antibodies. Unexpectedly, the data indicated that, in addition to Le^x and SLe^x, the heavy chain was also stained positive with anti-SLe^a serum. Although our MS/MS data on the major Fuc-containing biantennary N-glycans (Fig. 7) provided only convincing evidence for the SLe^x and Le^x linkages, it is possible that a very small amount of SLe^a is also present amongst the isomers, particularly on the multiantennary forms which were of low abundance and not subjected to further analysis. However, the monoclonal antibodies employed failed to bind both light chains, although the MS data clearly established the presence of at least Le^x and SLe^x on their N-glycans. It is possible that there is, overall, a much higher abundance of the implicated epitopes carried on the heavy chain, which contains five potential N-glycosylation sites relative to one each on the two light chains. The density of the presented epitopes would be further amplified by a higher abundance of multiantennary structures on the heavy chain.

Glycopeptide analyses

To seek information on the potential N-glycosylation site occupancies of the individual chains, tryptic peptides from each of the purified HC, LC1 and LC2 chains were subjected to automated nano-LC-nESI-MS/MS analyses, operated in a precursor ion discovery mode to optimize for glycopeptide detection. For the heavy chain, four distinct sets of glycopeptides were detected, corresponding to glycoforms of tryptic peptides carrying the N-glycosylated Asn28, Asn69, Asn163 and Asn183 residues (data not shown). The tryptic glycopeptide corresponding to the fifth potential site at Asn376 was not identified. The data are therefore consistent with a previous report, which estimated a total of four N-glycan chains carried on the heavy chain, based on partial PNGase F digestion and SDS-PAGE analysis [9,15]. There is apparently no strict preference for any particular complex-type N-glycan structure to be localized on any of the four sites, as most of the major structures found by MALDI-MS mapping of the released N-glycans could be detected amongst all four sets of glycopeptides observed. A more definitive quantification of each individual glycoform was not attempted as glycopeptides carrying some of the larger multiantennary structures are relatively minor and refractory to unambiguous identification by direct online LC-MS/MS analysis. Interestingly though, the single $Man_5GlcNAc_2$ structure could only be identified on Asn183.

For the light chains, tryptic glycopeptides carrying a single N-glycosylation site could be identified. Notably, the glycoform heterogeneity for LC1 was found to be less complex than that of LC2 (data not shown). Larger N-glycan structures extending up to $(Hex\text{-}HexNAc)_4$, with variable degrees of Fuc and Neu5Ac, were found only on LC2 and not on LC1, despite earlier

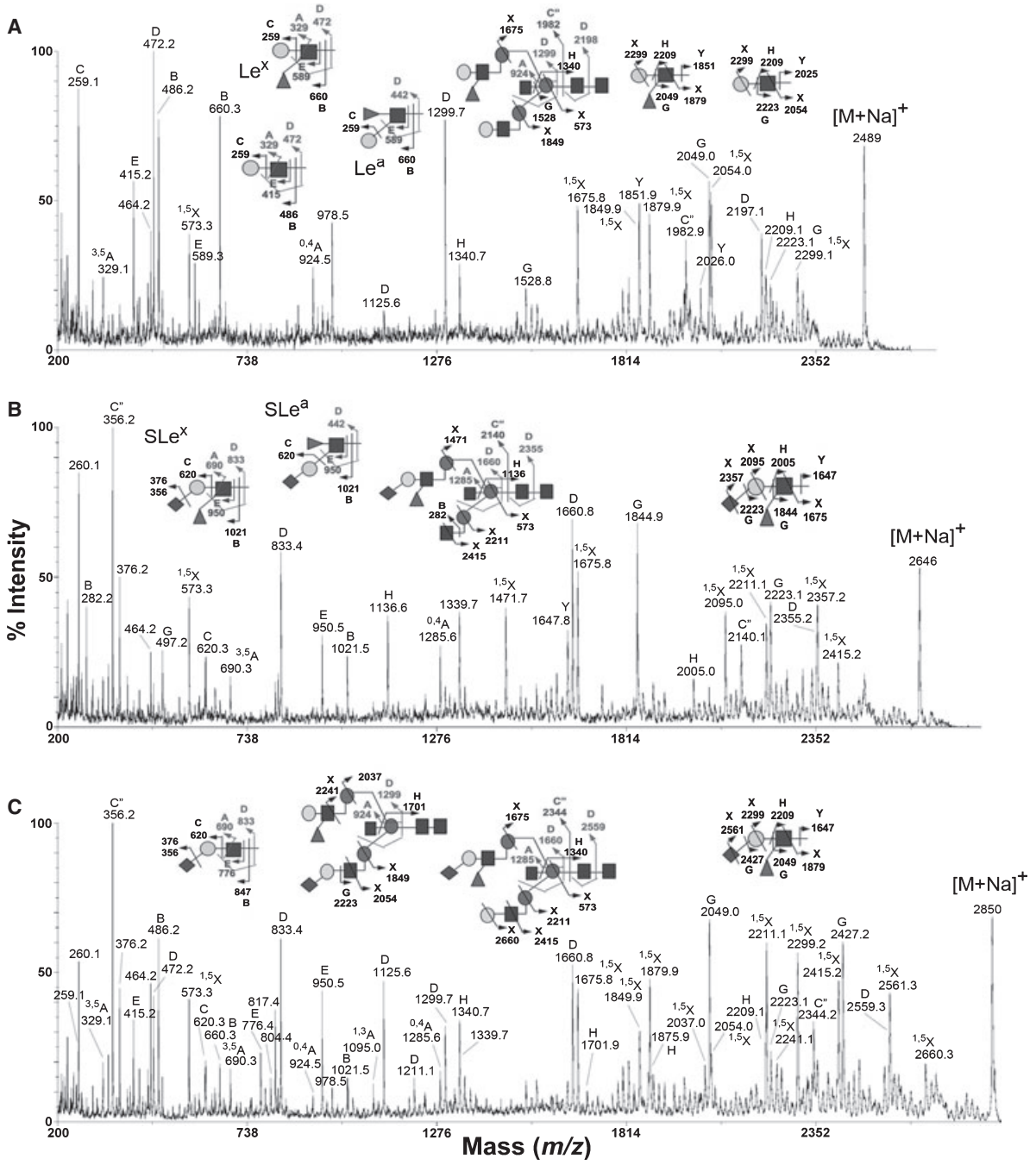

Fig. 7. MALDI-TOF/TOF MS/MS sequencing of Le^x- and SLe^x-containing N-glycans of RVV-X. The major N-glycans tentatively assigned as carrying the Lewis and sialyl-Lewis epitopes of interest (Table 1) were further subjected to MALDI-TOF/TOF MS/MS analysis to derive linkage-specific cleavage ions [40] for structural assignment. In general, the same molecular ion signals afforded by heavy and light chains gave similar MS/MS spectra, indicative of similar structures. Representative MS/MS spectra for the sodiated parent ions at *m/z* 2490, 2647 and 2851 (Fig. 6) are shown in (A), (B) and (C), respectively. For clarity of presentation, only the most abundant linkage and/or sequence informative ions are schematically illustrated and annotated. The nomenclature for the ion series follows that proposed by Domon and Costello [42] and Spina *et al.* [43], as adapted by Yu *et al.* [40]. Other nonannotated ions include: (1) a characteristic loss of 321 mass units from the D ions formed at bisected β-Man; (2) oxonium ions for terminal $HexNAc^+$ (*m/z* 260), $Neu5Ac^+$ (*m/z* 376) and $Hex\text{-}HexNAc^+$ (*m/z* 464). In (A) and (C), the presence of alternative isomers in which the nonfucosylated LacNAc is carried on the 6-arm is indicated by the D ion at *m/z* 1125. Symbols used: ◆, Neu5Ac; ▲, Fuc; ●, Hex (light-shaded for Gal and dark-shaded for Man, although these cannot be distinguished by MS analysis); ■, HexNAc (GlcNAc).

Table 1. Major RVV-X N-glycans detected by MS.

m/z[a]	Composition[b]	Deduced structure[c]
1579.5	H_5N_2	H_5N_2 (high mannose)
2275.1	H_6N_4	$(HN)_1$-H_2NC (hybrid)
N_2, $N_1(HN)_1$ or $(HN)_2$/biantennary complex		
1906.9	H_3N_5	N_2-NC
2111.0	H_4N_5	$N_1(HN)_1$-NC
2286.1	$F_1H_4N_5$	$F_1N_1(HN)_1$-NC
2647.2	$NeuAc_1F_1H_4N_5$	$NeuAc_1F_1N_1(HN)_1$-NC
2070.1	H_5N_4	$(HN)_2$C
2245.1	$F_1H_5N_4$	$F_1(HN)_2$-C
2316.1	H_5N_5	$(HN)_2$-NC
2419.2	$F_2H_5N_4$	$F_2(HN)_2$-C
2490.3	$F_1H_5N_5$	$F_1(HN)_2$-NC
2677.3	$NeuAc_1H_5N_5$	$NeuAc_1(HN)_2$-NC
2851.4	$NeuAc_1F_1H_5N_5$	$NeuAc_1F(HN)_2$-NC
3025.6	$NeuAc_1F_2H_5N_5$	$NeuAc_1F_2(HN)_2$-NC
3212.7	$NeuAc_2F_1H_5N_5$	$NeuAc_2F(HN)_2$-NC
$(HN)_3$/triantennary complex		
2520.3	H_6N_5	$(HN)_3$-C
2765.4	H_6N_6	$(HN)_3$-NC
2939.5	$F_1H_6N_6$	$F_1(HN)_3$-NC
3126.7	$NeuAc_1H_6N_6$	$NeuAc_1(HN)_3$-NC
3300.8	$NeuAc_1F_1H_6N_6$	$NeuAc_1F_1(HN)_3$-NC
3474.8	$NeuAc_1F_2H_6N_6$	$NeuAc_1F_2(HN)_3$-NC
3661.9	$NeuAc_2F_1H_6N_6$	$NeuAc_2F_1(HN)_3$-NC
3835.9	$NeuAc_2$ $F_2H_6N_6$	$NeuAc_2F_2(HN)_3$-NC
4198.1	$NeuAc_3F_2H_6N_6$	$NeuAc_3F_2(HN)_3$-NC
$(HN)_4$/tetra-antennary complex		
2969.5	H_7N_6	$(HN)_4$-C
3214.7	H_7N_7	$(HN)_4$-NC
3388.8	$F_1H_7N_7$	$F_1(HN)_4$-NC
3562.9	$F_2H_7N_7$	$F_2(HN)_4$-NC
3575.9	$NeuAc_1H_7N_7$	$NeuAc_1(HN)_4$-NC
3749.9	$NeuAc_1F_1H_7N_7$	$NeuAc_1F_1(HN)_4$-NC
3924.0	$NeuAc_1F_2H_7N_7$	$NeuAc_1F_2(HN)_4$-NC
3937.0	$NeuAc_2H_7N_7$	$NeuAc_2(HN)_4$-NC
4112.1	$NeuAc_2F_1H_7N_7$	$NeuAc_2F_1(HN)_4$-NC
4286.1	$NeuAc_2F_2H_7N_7$	$NeuAc_2F_2(HN)_4$-NC
4299.1	$NeuAc_3H_7N_7$	$NeuAc_3(HN)_4$-NC
4473.2	$NeuAc_1F_3H_7N_7$	$NeuAc_1F_3(HN)_4$-NC
4647.3	$NeuAc_3F_2H_7N_7$	$NeuAc_3F_2(HN)_4$-NC
$(HN)_5$/penta-antennary complex		
4026.0	$NeuAc_1F_2H_8N_8$	$NeuAc_1F_2(HN)_5$-NC
4374.2	$NeuAc_1F_2H_8N_8$	$NeuAc_1F_2(HN)_5$-NC
4561.3	$NeuAc_2F_1H_8N_8$	$NeuAc_2F_1(HN)_5$-NC
4736.4	$NeuAc_2F_2H_8N_8$	$NeuAc_2F_2(HN)_5$-NC

[a] Only major peaks are labelled and tabulated. *m/z* value refers to the accurate mass of the most abundant isotope peak. [b] Symbols used: F, Fuc; H, Hex (Man or Gal); N, HexNAc (GlcNAc). [c] Deduced structures based on the assumption that each of the *N*-glycans contains a trimannosyl core $Hex_3HexNAc_2$, denoted as -C, which is mostly bisected (-NC) and not fucosylated. MS/MS studies on selected peaks established that Fuc is mostly on the HexNAc of the nonreducing terminal Hex-HexNAc or LacNAc (Galβ1–4GlcNAc) sequence, and that a HexNAc-HexNAc- or LacdiNAc (GalNAcβ1–4GlcNAc-) terminal sequence was not detected amongst the major components. The LacNAc units are not fully sialylated and/or fucosylated, and thus give rise to heterogeneity in the distribution of the Le^x and SLe^x versus LacNAc and sialylated LacNAc terminal epitopes. The assigned tri-, tetra- and penta-antennary structures have not been verified by MS/MS, and may alternatively carry polyLacNAc sequences.

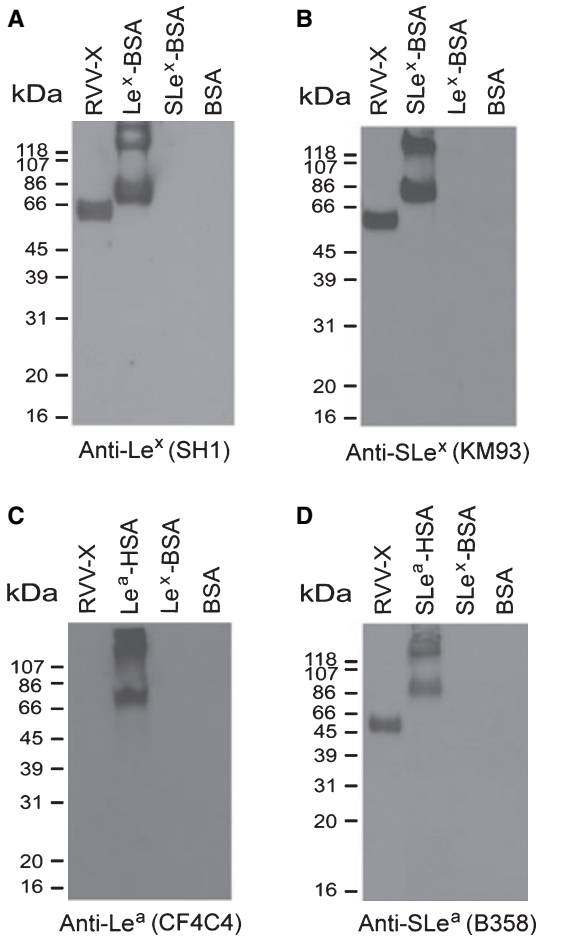

Fig. 8. Identification of Lewis epitopes on RVV-X using western blotting analyses. In each gel, 7 μg of RVV-X and 5 μg of BSA were loaded. Detections were performed with: (A) the Lewis x-specific antibody SH1; (B) the sialyl-Lewis x-specific antibody KM3; (C) the Lewis a-specific antibody CF4C4; and (D) the sialyl-Lewis a-specific antibody B358. Different dosages of Lewis-glycan-conjugated BSAs or human serum albumins were used as controls; the amounts loaded on to the gels were 3 μg in (A), 0.5 μg in (B) and 1 μg in (C) and (D).

mapping of the released N-glycans indicating a rather similar N-glycosylation profile for the two light chains. It is possible that these larger *N*-glycan structures, similar to those found on the heavy chain, are much less abundant relative to the major biantennary ones, and were not readily detectable without further glycopeptide purification and/or sample enrichment. The data are consistent with previous findings, which indicated that the mobility of LC2, but not of LC1, on SDS-PAGE was shifted noticeably with sialidase treatment [9]. This observation could be interpreted by the fact that LC2 carries a more elaborate N-glycosylation, with additional multisialylated and multiantennary structures not found on LC1, albeit of relatively low

abundance for each individual glycoform. In comparison, these larger structures occur at significantly higher abundance on the heavy chain and, with contribution from a total of four glycosylation sites, collectively present a high density and multivalency of the important terminal Le^x and SLe^x epitopes.

Functional significance of the glycans in venom proteins

Previous studies have suggested that the trimannosyl sugar cores are sufficient for the maintenance of the conformation and *in vitro* enzymatic activity of RVV-X [15], but have not addressed the *in vivo* contribution of its glycans. We also added neuraminidase to remove the terminal sialic acid residues from the glycans in RVV-X, and the modified protein moved faster in the electrophoresis gel, as expected (Fig. 9A). By APTT assays, we found that the coagulating activity of RVV-X was decreased slightly (by 5%) after sialidase treatment (Fig. 9B). This is consistent with previous results, which showed that RVV-X remained active after treatment with various exoglycosidases [15].

Markedly elevated fibrinogen degradation product (FDP) concentrations have been observed frequently in the blood of patients affected by Russell's viper bites, indicating the activation of fibrinolysis and systemic envenomation [26,27]. We thus compared the effects of native and desialylated RVV-X on the plasma FDP level in ICR mice using an immunochemical kit. As shown in Fig. 9C, the serum FDP levels were elevated within 1–8 h after intraperitoneal injection of a dose of 1.0 $\mu g \cdot g^{-1}$ of native RVV-X. In contrast, mice injected with desialylated RVV-X showed a slower and 30–40% smaller FDP increment relative to those injected with native RVV-X. As SLe^x and SLe^a epitopes present on RVV-X molecules (Figs 7 and 8) can bind specifically to E- and P-selectins of activated endothelial cells or platelets [28,29], removal of sialic acid from RVV-X possibly abolishes or slows down its homing and localization to the vascular system and the generation of FDP.

We have also tested the lethal potency of RVV-X to ICR mice by different routes of injection. The LD_{50} value of intravenous injection (0.04 $\mu g \cdot g^{-1}$ mouse) was about 50 times lower than that of intraperitoneal injection (2.0 $\mu g \cdot g^{-1}$ mouse), and intravenous injection resulted in prominent systemic haemorrhage in mice. These results emphasize the importance of the rapid homing of RVV-X into microvessels to exert its effect. The glycan structures of a number of venom glycoproteins have been characterized previously. The L-amino acid oxidase of Malayan pitviper venom contains bis-sialylated N-glycans, which possibly mediate binding to the cell surface and cause subsequent internalization [30,31]. For cobra venom factor, the terminal α-galactosyl residues of its N-glycans have been shown to prevent its Le^x-dependent uptake and clearance by the liver [32,33]. Thus, it appears that sugars play important roles in venom toxicology, not only by increasing the solubility and stability of venom glycoproteins, but also by promoting their target recognition and specific binding *in vivo*.

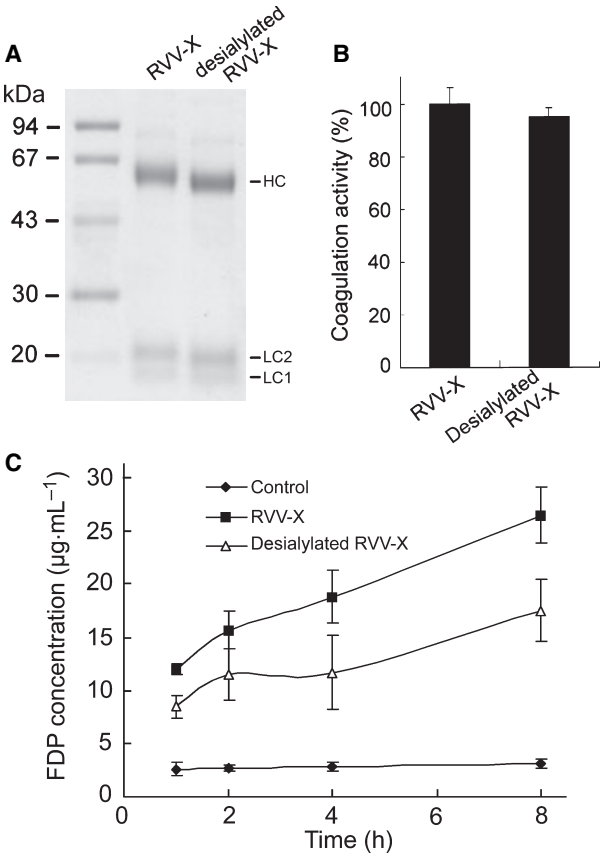

Fig. 9. Effect of RVV-X desialylation on FDP induction. (A) SDS-PAGE analysis of desialylated RVV-X. (B) Comparison of the *in vitro* coagulation activities between native and desialylated RVV-X. (C) Time course of induced FDP elevation. ICR mice were injected (intraperitoneally) with either native or desialylated RVV-X at a dose of 1.0 $\mu g \cdot g^{-1}$ body weight. The plasma FDP level in each sample was determined after different times. The results are expressed as the mean ± standard deviation (n = 3).

Conclusions

By far-western analyses, we have shown that RVV-X strongly binds protein S in addition to factors X and IX under millimolar Ca^{2+} ion concentrations. We have

also cloned and solved the complete sequences of the three subunits of RVV-X from *D. siamensis* venom. The newly sequenced LC2 belongs to the A-chain subfamily of venom C-lectin-like proteins and has one N-glycosylation site and an extra Cys135 residue linking to the RVV-X heavy chain. Moreover, *N*-glycan profiling revealed the presence of Le and SLe epitopes on RVV-X, which have specific binding receptors on platelets and endothelial cells. The important role of these glycans in pharmacokinetics has been demonstrated by the slower and smaller increment of FDP *in vivo* after the injection of desialylated RVV-X rather than intact RVV-X. As both RVV-X and RVV-V [34] are procoagulating glycoproteins in the same venom, the common glycosylation system in the endoplasmic reticulum Golgi of venom glands presumably generates similar multivalent glycoepitopes in these glycoproteins. It is probable that these glycoepitopes may be responsible for the cohoming of both venom enzymes to the vascular system of the envenomated victims and for the activation of prothrombin synergistically.

Experimental procedures

Materials

Human coagulation factor X, Gla-domainless factor X, prothrombin, protein C and protein S were purchased from Haematologic Technologies Inc. (Essex, VT, USA). Factor IX was obtained from Baxter Healthcare Corp. (Fremont, CA, USA). The anti-Le^x (SH1) and anti-Le^a (CF4C4) IgG were purchased from GlycoNex Inc. (Taipei, Taiwan). The anti-SLe^x (KM93) and anti-SLe^a (B358) IgM were obtained from Chemicon (Temacula, CA, USA) and Biomeda (Foster City, CA, USA), respectively. For immunochemical detection, a horseradish peroxidase-conjugated goat anti-mouse IgG or IgM secondary serum was purchased from Bethyl Laboratories Inc. (Montgomery, TX, USA). Le^x-BSA and SLe^x-BSA were obtained from Calbiochem (Schwalbach, Germany); SLe^a-human serum albumin was purchased from GlycoTech Corp. (Gaithersburg, MD, USA). To prepare Le^a glycan epitope (used as a positive control for anti-Le^a specific IgG), 1 mg·mL^{-1} SLe^a-human serum albumin in 50 mM sodium acetate, pH 5.5 was treated with neuraminidase (Roche Diagnostics, Mannheim, Germany) overnight to remove terminal sialic acids.

Purification of RVV-X

RVV-X was isolated from venom as described previously [16] with minor modifications. About 20 mg of *D. siamensis limitus* venom (Venom Supplies, Adelaide, Australia) was dissolved in 200 μL of 0.1 M ammonium acetate (pH 6.7) and loaded onto a Superdex G-75 column (10/300 GL; Pharmacia, Uppsala, Sweden) on an FPLC apparatus. The column was eluted at a flow rate of 1.0 mL·min^{-1}, and fractions of 0.5 mL were collected. After assay for coagulation activity, the active fractions were pooled, dialysed, and lyophilized. The pooled fraction was further loaded onto a Mono Q column (5/50 GL; Pharmacia) which had been pre-equilibrated with 50 mM Tris/HCl buffer (pH 8.0), and eluted with a two-step gradient of NaCl (0–0.6 M). Protein concentrations were measured by the bicinchoninic acid protein assay (Pierce Chemical Co., Rockford, IL, USA) using BSA as a standard.

N-terminal sequencing of LC2

Purified RVV-X (10–20 μg per well) was subjected to SDS-PAGE on a 1.0-mm-thick 12% gel under reducing conditions. The protein bands were electroblotted to a PVDF membrane. After staining with Amido Black (0.2% in 7% acetic acid), the band corresponding to LC2 was excised and sequenced using a gas-phase amino acid sequencer Procise 492 (Applied Biosystems, Foster City, CA, USA).

Coagulation assay

APTT assays were carried out on an automatic coagulation analyser (Hemostasis Analyzer KC-1; Sigma Diagnostics, St Louis, MO, USA) according to the manufacturer's protocol. Briefly, 50 μL of human plasma was incubated with 5 μL of sample at 37 °C for 1 min. Then, 50 μL of Alexin® (purified rabbit brain cephalin) was added and incubated for 1.5 min. Finally, a 50 μL aliquot of $CaCl_2$ (20 mM) was added to trigger coagulation, and the clotting time was recorded automatically by the analyser.

Stability of RVV-X at different temperatures and buffer pH values

Different doses of RVV-X (0.1, 0.5, 1, 5 and 10 ng) were first tested by coagulation assay to establish a calibration curve for data evaluation. To study its thermal stability, RVV-X (1.0 μg·μL^{-1}) in 100 mM Hepes (pH 8.0) was incubated at −20, 4, 25, 37, 50, 60, 70 and 80 °C for 60 min. In addition, RVV-X (1.0 μg·μL^{-1}) was incubated at 4 °C for 36 h in 100 mM of various buffers, including sodium acetate (pH 3–5), Hepes (pH 6–8) and glycine/NaOH (pH 9–11). The remaining activity of 5 ng of RVV-X was determined by measuring the clotting time on a coagulation analyser.

Biotinylation of RVV-X and far-western blotting

The BiotinTag™ Micro-Biotinylation Kit (Sigma-Aldrich Co., St Louis, MO, USA) was used; 0.6 mg of purified RVV-X in 0.1 mL of 0.1 M phosphate buffer (pH 7.2) was mixed with 10 mL of BAC-sulfoNHS solution (5 mg·mL^{-1}

in 0.1 M phosphate buffer) and incubated with gentle stirring for 30 min at room temperature. The biotinylated protein was desalted by a Microspin G-50 column pre-equilibrated with $NaCl/P_i$, and stored at −20 °C until use.

Various human coagulation factors were subjected to SDS-PAGE on an 8% gel under nonreducing conditions. Protein bands in the gel were transferred to a PVDF membrane, followed by incubation for 1 h in blocking solution [1% BSA in Tris-buffered saline with Tween 20 (TBST: 20 mM Tris/HCl, pH 8.0, 150 mM NaCl and 0.1% Tween 20)]. Subsequently, the membrane was incubated in TBST with 1.5 $\mu g \cdot mL^{-1}$ biotinylated RVV-X for 1 h at 25 °C. After three 5 min washes with TBST, bound biotinylated RVV-X was probed by the addition of a 1 : 1000-diluted SBHP system in TBST for 1 h, and developed with a solution containing 0.1 $mg \cdot mL^{-1}$ 3,3′-diaminobenzidine, 0.25% $NiCl_2$ and 0.05% H_2O_2 in NaCl/Tris. For experiments in the presence of Ca^{2+} ions, 5 mM $CaCl_2$ was included in the TBST solution in each step.

Cloning and sequencing

The venom gland mRNA and cDNA were prepared from *D. siamensis limitus*, as described previously [35]. Two pairs of primers corresponding to the conserved 5′ signal peptide and 3′ noncoding region were designed based on the cDNA sequences of snake venom C-type lectin proteins and metalloproteases [36,37], and used to amplify specific cDNA by PCR. For cloning of LC1and LC2, the sense primer was 5′-GGAA(C/G)GAAG(A/G)CCATGGGGCG-3′ and the antisense primer was 5′-CTTC(C/T)TTGCTTCTC CA(A/G)ACTTC-3′. For cloning of the heavy chain, the sense primer was 5′-GCCAAAT(C/T)CAGCCTCCAAA ATG-3′ and the antisense primer was 5′-CTGAGAGA AGCCAGTGGTTGA-3′. To clone its far 3′ noncoding region, the sense primer (a 20-mer designed from sequence PRDQLQQ of the disintegrin domain) and antisense primer (an 18-mer based on its far 3′ end UTR) were used. The PCR conditions were as follows: an initial denaturation at 94 °C for 2 min, followed by 35 cycles of extension (72 °C, 1 min), denaturation (94 °C, 1 min) and annealing (52 °C, 1 min), and a terminal extension at 72 °C for 10 min. After PCR, the products were cloned into the pGEM-T easy vector (Promega Corp., Madison, WI, USA) and transformed to *Escherichia coli* strain JM 109. The white transformants were screened and the positives were subjected to sequencing on a DNA Sequencing System Model 373A and Taq-Dye-Deoxy Terminator Cycle Sequencing Kit (Applied Biosystems).

Preparation of glycopeptides and release of *N*-glycans for MS analysis

RVV-X in 50 mM ammonium bicarbonate (pH 8.4) was first reduced with dithiothreitol at 37 °C for 1 h, and then alkylated with iodoacetamide at room temperature for 1 h in the dark, followed by the removal of excess reagents by passing through a Sep-Pak C8 cartridge. For glycosylation site analysis, the reduced alkylated sample was digested with sequencing-grade modified trypsin (Promega Corp.), and the resulting glycopeptide and peptide mixtures were analysed directly by LC-MS/MS. For *N*-glycan analysis, the sample was digested sequentially with trypsin (Sigma) and chymotrypsin (Sigma) at 37 °C for 4 h each. After brief boiling and cooling, the glycopeptide and peptide mixtures were incubated with PNGase F (Roche Diagnostics) overnight at 37 °C, and then passed through a C18 Sep-Pak cartridge (Waters Co., Milford, MA, USA) in 5% acetic acid, as described previously [38].

Desialylation and enzyme digestion for MS analysis

Desialylation was performed by digestion with 50 mU of *Macrobdella decora* α2,3 neuraminidase (Calbiochem) in 20 μL of 50 mM sodium acetate buffer, pH 6.0, at 37 °C overnight. Further removal of β-Gal from desialylated N-glycans was performed with β4-specific galactosidase of *Streptococcus pneumoniae* (Calbiochem) in 100 μL of 50 mM sodium acetate buffer, pH 5.5, at 37 °C for 12 h.

MALDI-MS and MS/MS analysis

All glycans were permethylated using a modified NaOH/dimethylsulfoxide method [38], originally described by Ciucanu and Kerek [39], prior to MS analysis. For MALDI-TOF MS glycan profiling, the permethyl derivatives in acetonitrile were mixed 1 : 1 with 2,5-dihydroxybenzoic acid matrix (10 $mg \cdot mL^{-1}$ in acetonitrile), spotted on to the target plate, air dried and recrystallized on the plate with acetonitrile. Data acquisition was performed manually on a benchtop MALDI LR system (Micromass, Manchester, UK) operated in the reflectron mode. MALDI-MS/MS sequencing of the permethylated glycans was performed on both a Q-TOF Ultima MALDI (Waters Micromass, Manchester, UK) and 4700 Proteomics Analyzer (Applied Biosystems), exactly as described previously [40].

LC-MS/MS analysis of glycopeptides

Online nanoLC-nanoESI-MS/MS analyses of the tryptic peptides/glycopeptides from RVV-X were performed on a Micromass Q-TOF Ultima API mass spectrometer fitted with a nano-LC sprayer, a PepMap C18 m-precolumn cartridge (5 μm, 300 μm internal diameter × 5 mm; Dionex, Sunnyvale, CA, USA) and an analytical C18 capillary column (15 cm × 75 μm internal diameter, packed with 5 μm Zorbax 300 SB C18 particles; Micro-Tech Scientific, Vista, CA, USA) at a flow rate of 300 $nL \cdot min^{-1}$ using a 60 min gradient of 5–80% acetonitrile in 0.1% formic acid. To

facilitate the identification of glycopeptides, automated MS/MS data-dependent acquisition was operated under the precursor ion discovery mode [41]. In brief, alternate low (7 eV) and high (30 eV) collision energy LC-MS survey scans were employed to trigger MS/MS acquisition on the five most intense parent ions observed during the low-energy survey scans, when glycan-specific oxonium ion fragments, m/z 204.084 for $HexNAc^+$ and m/z 366.139 for $HexHexNAc^+$, were detected at the corresponding high-energy scans. MS/MS acquisition on false positives was limited to a single scan if the monitored oxonium ions were not afforded, so as to devote more analysis time to true positives.

Western blotting analyses of the glycan epitopes

Samples of 7 μg of RVV-X and 5 μg of BSA were analysed by 8% SDS-PAGE under reducing conditions. Appropriate amounts of $Le^{x/a}$- and $SLe^{x/a}$-conjugated BSAs and human serum albumins were used as controls. After blotting onto a PVDF membrane, immunoblotting was carried out using anti-$Le^{x/a}$ and $SLe^{x/a}$ serum (1 : 1000 dilution) and horseradish peroxidase-conjugated second antibody (1 : 2000 dilution). Positive bands were detected using enhanced chemiluminescent reagents (Pharmacia).

Desialylation and FDP measurement

To remove the terminal sialic acids, 120 μg of RVV-X was treated with 25 mU of *Vibrio cholerae* α2,3 neuraminidase (Roche) in 120 μL of 50 mM Hepes (pH 7.0) at 37 °C for 4 h. The modification was confirmed by analysis of the product using SDS-PAGE.

The concentration of FDP was determined using the NANOPIA P-FDP Kit (Daiichi Pure Chemicals Co., Tokyo, Japan). At different times after intraperitoneal injection of RVV-X, ICR mouse blood was collected in sodium citrate (9 : 1, v/v) and centrifuged at 1000 ***g*** at room temperature for 10 min. The FDP concentration in mouse plasma was measured following the manufacturer's procedure. Briefly, 8 μL of the plasma was incubated with 130 μL of P-FDP buffer at 37 °C for 5 min. After mixing with 130 μL of Latex Reagent, the absorbance was measured immediately at 570 nm. The reaction was further incubated at 37 °C for 5 min, and the absorbance was measured at 800 nm. The FDP concentration of each sample was determined from a calibration curve, which was established by differences between the absorbance at 570 and 800 nm versus the different concentrations of standard FDP products (7.5, 14.3, 30, 60 and 120 $\mu g \cdot mL^{-1}$).

Acknowledgements

We thank Ms Ying-Ming Wang for supplying venom cDNA and Mr Sz-Wei Wu for the MALDI-TOF/TOF MS/MS analyses of sugars. Mass spectrometry data were acquired at the NRPGM Core Facilities for Proteomics, Academia Sinica, supported by a National Science Council grant (94-3112-B-001-009-Y). This research was also supported by grants from Academia Sinica and the National Science Council, Taiwan.

References

1 Yamada D, Sekiya F & Morita T (1998) Prothrombin and factor X activator activities in the venoms of Viperidae snakes. *Toxicon* **35**, 1581–1589.
2 Kini RM (2005) The intriguing world of prothrombin activators from snake venom. *Toxicon* **45**, 1133–1145.
3 Zhang Y, Xiong YL & Bon C (1995) An activator of blood coagulation factor X from the venom of *Bungarus fasciatus*. *Toxicon* **33**, 1277–1288.
4 Morita T (1998) Proteases which activate factor X. In *Enzymes From Snake Venom* (Bailey GS, ed.), pp. 179–208. Alaken, Fort Collins, CO.
5 Jackson CM & Nemerson Y (1980) Blood coagulation. *Annu Rev Biochem* **49**, 765–811.
6 Lindquist PA, Fujikawa K & Davie EW (1978) Activation of bovine factor IX (Christmas factor) by factor XIa (activated plasma thromboplastin antecedent) and a protease from Russell's viper venom. *J Biol Chem* **253**, 1902–1909.
7 Tans G & Rosing J (2001) Snake venom activators of factor X: an overview. *Haemostasis* **31**, 225–233.
8 Takeya H, Nishida S, Miyata T, Kawada S, Saisaka Y, Morita T & Iwanaga S (1992) Coagulation factor X activating enzyme from Russell's viper venom (RVV-X). A novel metalloproteinase with disintegrin (platelet aggregation inhibitor)-like and C-type lectin domains. *J Biol Chem* **267**, 14109–14117.
9 Gowda DC, Jackson CM, Hensley P & Davidson EA (1994) Factor X-activating glycoprotein of Russell's viper venom. Polypeptide composition and characterization of the carbohydrate moieties. *J Biol Chem* **269**, 10644–10650.
10 Fox JW & Serrano SM (2005) Structural considerations of the snake venom metalloproteinases, key members of the M12 reprolysin family of metalloproteinases. *Toxicon* **45**, 969–985.
11 Atoda H, Yoshida N, Ishikawa M & Morita T (1994) Binding properties of the coagulation factor IX/factor X-binding protein isolated from the venom of *Trimeresurus flavoviridis*. *Eur J Biochem* **224**, 703–708.
12 Takeda S, Igarashi T & Mori H (2007) Crystal structure of RVV–X: an example of evolutionary gain of specificity by ADAM proteinases. *FEBS Lett* **581**, 5859–5864.
13 Siigur E, Tonismagi K, Trummal K, Samel M, Vija H, Subbi J & Siigur J (2001) Factor X activator from

Vipera lebetina snake venom, molecular characterization and substrate specificity. *Biochim Biophys Acta* **1568**, 90–98.
14 Siigur E, Aaspollu A, Trummal K, Tonismagi K, Tammiste I, Kalkkinen N & Siigur J (2004) Factor X activator from *Vipera lebetina* venom is synthesized from different genes. *Biochim Biophys Acta* **1702**, 41–51.
15 Gowda DC, Jackson CM, Kurzban GP, McPhie P & Davidson EA (1996) Core sugar residues of the *N*-linked oligosaccharides of Russell's viper venom factor X-activator maintain functionally active polypeptide structure. *Biochemistry* **35**, 5833–5837.
16 Kisiel W, Hermodson MA & Davie EW (1976) Factor X activating enzyme from Russell's viper venom: isolation and characterization. *Biochemistry* **15**, 4901–4906.
17 Masuda S, Hayashi H & Araki S (1998) Two vascular apoptosis-inducing proteins from snake venom are members of the metalloprotease/disintegrin family. *Eur J Biochem* **253**, 36–41.
18 Skogen WF, Bushong DS, Johnson AE & Cox AC (1983) The role of the Gla domain in the activation of bovine coagulation factor X by the snake venom protein XCP. *Biochem Biophys Res Commun* **111**, 14–20.
19 Mizuno H, Fujimoto Z, Atoda H & Morita T (2001) Crystal structure of an anticoagulant protein in complex with the Gla domain of factor X. *Proc Natl Acad Sci USA* **98**, 7230–7234.
20 Dahlback B (1995) The protein C anticoagulant system: inherited defects as basis for venous thrombosis. *Thromb Res* **77**, 1–43.
21 Hackeng TM, Sere KM, Tans G & Rosing J (2006) Protein S stimulates inhibition of the tissue factor pathway by tissue factor pathway inhibitor. *Proc Natl Acad Sci USA* **103**, 3106–3111.
22 Mizuno H, Fujimoto Z, Koizumi M, Kano H, Atoda H & Morita T (1997) Structure of coagulation factors IX/X-binding protein, a heterodimer of C–type lectin domains. *Nat Struct Biol* **4**, 438–441.
23 Atoda H, Kaneko H, Mizuno H & Morita T (2002) Calcium-binding analysis and molecular modeling reveal *Echis* coagulation factor IX/factor X-binding protein has the Ca-binding properties and Ca ion-independent folding of other C-type lectin-like proteins. *FEBS Lett* **531**, 229–234.
24 Kishimoto M & Takahashi T (2002) Molecular cloning of HR1a and HR1b, high molecular hemorrhagic factors, from *Trimeresurus flavoviridis* venom. *Toxicon* **40**, 1369–1375.
25 Takeda S, Igarashi T, Mori H & Araki S (2006) Crystal structures of VAP1 reveal ADAMs' MDC domain architecture and its unique C-shaped scaffold. *EMBO J* **25**, 2388–2396.
26 Than-Than, Hutton RA, Myint-Lwin, Khin-Ei-Han, Soe-Soe, Tin-Nu-Swe, Phillips RE & Warrell DA (1988) Haemostatic disturbances in patients bitten by Russell's viper (*Vipera russelli siamensis*) in Burma. *Br J Haematol* **69**, 513–520.
27 Li QB, Yu QS, Huang GW, Tokeshi Y, Nakamura M, Kinjoh K & Kosugi T (2000) Hemostatic disturbances observed in patients with snakebite in south China. *Toxicon* **38**, 1355–1366.
28 Kannagi R, Izawa M, Koike T, Miyazaki K & Kimura N (2004) Carbohydrate-mediated cell adhesion in cancer metastasis and angiogenesis. *Cancer Sci* **95**, 377–384.
29 Furie B & Furie BC (2004) Role of platelet P-selectin and microparticle PSGL-1 in thrombus formation. *Trends Mol Med* **10**, 171–178.
30 Geyer A, Fitzpatrick TB, Pawelek PD, Kitzing K, Vrielink A, Ghisla S & Macheroux P (2001) Structure and characterization of the glycan moiety of L-amino-acid oxidase from the Malayan pit viper *Calloselasma rhodostoma*. *Eur J Biochem* **268**, 4044–4053.
31 Ande SR, Kommoju PR, Draxl S, Murkovic M, Macheroux P, Ghisla S & Ferrando-May E (2006) Mechanisms of cell death induction by L-amino acid oxidase, a major component of ophidian venom. *Apoptosis* **11**, 1439–1451.
32 Gowda DC, Glushka J, Halbeek H, Thotakura RN, Bredehorst R & Vogel CW (2001) *N*-linked oligosaccharides of cobra venom factor contain novel (1–3) galactosylated Le^x structures. *Glycobiology* **11**, 195–208.
33 Fu Q, Satyaswaroop PG & Gowda DC (1997) Tissue targeting and plasma clearance of cobra venom factor in mice. *Biochem Biophys Res Commun* **231**, 316–320.
34 Tokunaga F, Nagasawa K, Tamura S, Miyata T, Iwanaga S & Kisiel W (1988) The factor V-activating enzyme (RVV–V) from Russell's viper venom. *J Biol Chem* **263**, 17471–17481.
35 Wang YM, Lu PJ, Ho CL & Tsai IH (1992) Characterization and molecular cloning of neurotoxic phospholipases A_2 from Taiwan viper (*Vipera russelli formosensis*). *Eur J Biochem* **209**, 635–641.
36 Harrison RA, Oliver J, Hasson SS, Bharati K & Theakston RD (2003) Novel sequences encoding venom C–type lectins are conserved in phylogenetically and geographically distinct *Echis* and *Bitis* viper species. *Gene* **315**, 95–102.
37 Tsai IH, Wang YM, Chiang TY, Chen YL & Huang RJ (2000) Purification, cloning and sequence analyses for pro-metalloprotease-disintegrin variants from *Deinagkistrodon acutus* venom and subclassification of the small venom metalloproteases. *Eur J Biochem* **267**, 1359–1367.
38 Dell A, Reason AJ, Khoo KH, Panico M, McDowell RA & Morris HR (1994) Mass spectrometry of carbohydrate-containing biopolymers. *Methods Enzymol* **230**, 108–132.

39 Ciucanu I & Kerek F (1984) A simple and rapid method for the permethylation of carbohydrates. *Carbohydr Res* **131**, 209–217.
40 Yu SY, Wu S & Khoo KH (2006) Distinctive characteristics of MALDI-Q/TOF and TOF/TOF tandem mass spectrometry for sequencing of permethylated complex type *N*-glycans. *Glycoconj J* **23**, 355–369.
41 Ritchie MA, Gill AC, Deery MJ & Lilley K (2002) Precursor ion scanning for detection and structural characterization of heterogeneous glycopeptide mixtures. *J Am Soc Mass Spectrom* **13**, 1065–1077.
42 Domon B & Costello CE (1988) A systematic nomenclature for carbohydrate fragmentations in FAB-MS/MS spectra of glycoconjugates. *Glycoconj J* **5**, 397–409.
43 Spina E, Sturiale L, Romeo D, Impallomeni G, Garozzo D, Waidelich D & Glueckmann M (2004) New fragmentation mechanisms in matrix-assisted laser desorption/ionization time-of-flight/time-of-flighttandem mass spectrometry of carbohydrates. *Rapid Commun Mass Spectrom* **18**, 392–398.